GPPF-2017-29

LARGE EDDY SIMULATION OF A LIQUID JET IN CROSSFLOW USING A QUASI MULTIPHASE EULERIAN APPROACH FOR ATOMIZATION MODELLING

Stefano Puggelli
Department of Industrial Engineering (DIEF)
University of Florence
stefano.puggelli@htc.de.unifi.it
Florence, Italy

Antonio Andreini
Department of Industrial Engineering (DIEF)
University of Florence
antonio.andreini@htc.de.unifi.it
Florence, Italy

Lorenzo Mazzei
Department of Industrial Engineering (DIEF)
University of Florence
lorenzo.mazzei@htc.de.unifi.it
Florence, Italy

François-Xavier Demoulin
CNRS CORIA UMR 6614
University of Rouen
demoulin@coria.fr
Rouen, France

ABSTRACT

The increasingly strict regulations in terms of pollutant emissions imposed in aero-engine framework is forcing to a drastic reduction of NOx levels with respect to the current Rich Quench Lean (RQL) design, leading to the adoption of lean combustion systems. Such burning mode is characterized by the use of highly swirled flows for flame stabilization. This can lead to aeroacoustics instabilities and pressure fluctuations and therefore to performances highly related to the evolution of the liquid atomization process. Therefore, on a numerical point of view scale resolved approaches such as Large Eddy Simulation (LES) are required in conjunction with proper models for liquid phase handling in order to properly appreciate such complex phenomena. To this end, considering the well-known drawbacks of standard Eulerian-Lagrangian (E-L) approaches in terms of computational costs in LES framework, the attention in the last years has been focused on Eulerian-Eulerian (E-E) methods.

In the present work, LES simulations of a water jet in air crossflow have been performed using the Quasi Multiphase Eulerian (QME) approach for liquid phase modelling. The QME model is an extension of the E-E solver derived from the Eulerian Lagrangian Spray Atomization (ELSA) concept based on the addition of a transport equation for the turbulent liquid flux to account for slip velocity effects. Numerical results have been compared with the available experimental data in terms of both mean penetration and its standard deviation, as well as LES results obtained with ELSA and with a standard Volume of Fluid (VoF) approach. All the simulations have been realized using OpenFoam 3.0.1.

The results highlight the capabilities of QME in predicting the main characteristics of the analysed jet in crossflow leading to noticeable enhancements with respect to ELSA in terms of liquid penetration and to a lower computational cost with respect to a VoF approach.

INTRODUCTION

The future standards on pollutants emissions expected by ICAO-CAEP [1] standards for the next generation of civil aero-engines have pushed the attention towards the introduction of lean burn technology in aeronautical framework. Here, a drastic reduction of NOx levels can be achieved working on a narrow range of temperature and equivalence ratio. Therefore, all the issues related to liquid fuel atomization and air-fuel mixing have to be carefully investigated and CFD simulations have been gaining strong attention for the design process.

However, because of the highly swirled and turbulent flow-field typical of lean combustors, numerical simulations are moving towards an extensive use of scale resolved techniques such as Large Eddy Simulation (LES) or hybrid RANS-LES models. In this framework, the numerical method chosen for the modelling of the liquid phase can have a strong impact on both the simulation accuracy and the computational effort. Indeed, the lagrangian approach, which is based on tracking single liquid discrete entities (i.e. parcels), is normally characterized by CPU costs above levels for industrial applications on a scale resolved context and it presents limited capabilities in terms of numerical vectorization and parallelization.

Besides, Eulerian-Eulerian (E-E) methods are very attractive since several ways, associated to different computational costs, can be used to solve the kinetic Boltzmann-Williams equation (Williams [2]). This has determined a copious research on Eulerian methods starting from approaches based on a discretization of the spray distribution along the diameter space (i.e. sectional

approaches) (Laurent and Massot [3]) to other built on the calculation of some moments of the spray probability density function (such as Quadrature Method Of Moments (Marchisio et al. [4]) or Direct Quadrature Method Of Moments (Fox et al. [5])). Recent contributions in this area have shown the suitability of these methods in describing the most important features of liquid sprays (Massot [6], Vié et al. [7]). Nevertheless, since all these approaches are theoretically based on the Boltzmann-Williams equation, they can be only used when a dilute spray is generated whereas during the atomization process the liquid phase is initially a continuum. Such shortcoming determines an extensive use of experimental correlations in order to introduce the effects of primary breakup inside the numerical calculations. However, this strategy is not general since a strong spreading between the huge number of available experimental correlations can be determined for the same configuration and operating conditions.

To overcome these limitations, in this work, a Quasi Multiphase Eulerian (QME) approach (Andreini et al. [8]) has been used to reconstruct the atomization process of the turbulent liquid jet in a subsonic gas crossflow experimentally studied in Brown and McDonell [9]. Such approach is an extension of the E-E solver derived from the ELSA concept (Vallet and Borghi [10]), based on the addition of a transport equation for turbulent liquid flux inside the liquid volume fraction equation. The model, exploiting the equation for the liquid/gas interface density derived for ELSA, is directly applicable both in the dense and disperse spray zone. Moreover, it can be directly employed to study the primary breakup region where lagrangian and various E-E approaches are not theoretically valid. Indeed, in the present work the selection of a jet in crossflow configuration has been realized in order to study a relevant application from an engineering point of view where both primary breakup and a disperse spray can be determined.

The focus here is the assessment of the predictive capabilities of such QME approach in LES framework with respect to ELSA and against a standard Volume of Fluid (VoF) approach. All the calculations have been realized using OpenFoam 3.0.1

The paper is structured as follow: the first part is devoted to the description of the experimental test case and to the characterization of the mathematical models used to describe the liquid atomization process. In the second part, the obtained numerical results are compared against experimental data focusing the attention on the near injector region.

DESCRIPTION OF THE TEST CASE

The test case under investigation is the water jet in a subsonic air crossflow experimentally studied in Brown and McDonell [9]. The main features of the experimental setup are reported in Figure 1, whereas a more detailed description of the test article can be found in Andreini et al. [8] and in Brown and McDonell [9]. A long pipe of 7.49 mm is

followed by a 118 angled taper section and by a short pipe of length L with a diameter d=1.30 mm and L/d=4.

The experimental apparatus was designed to give a detailed description of a water injection in an air crossflow for several values of the momentum flux ratio $\left(q = \frac{\rho_j U_j^2}{\rho_c U_c^2}\right)$ and crossflow Weber number $\left(We_c = \frac{\rho_c U_c^2 d_j}{\sigma}\right)$ to achieve an insight of the transition between "column" to "surface-dominated" breakup type. In the present study, the test point characterized by the operating conditions described in Table 1 has been simulated.

A high-speed video camera was used in order to analyse the jet behaviour giving information in terms of both global jet breakup mechanisms (see Figure 1) as well as mean penetration and its standard deviation (green and red curves respectively superimposed on the experimental picture).

The experiments are focused on the near injector region (8 liquid jet diameters after jet exit) and no experimental data have been provided yet for the subsequent spray generation.
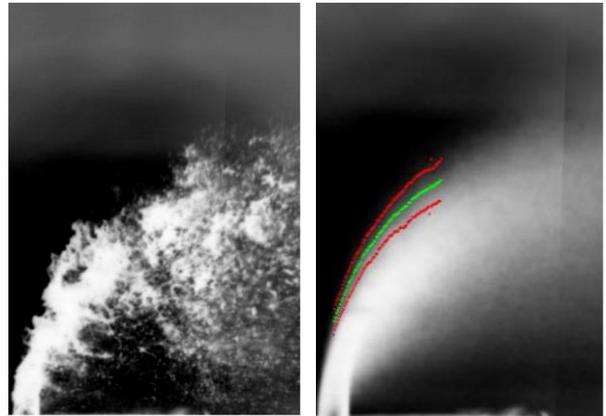

Figure 1: Visualization of the jet breakup in the operating conditions of interest (taken from Brown and McDonell [9]) .

Table 1: Operating conditions for the test point.

Momentum Flux Ratio (q)	6.6
Crossflow Weber number (We$_c$)	330
Jet Weber number (We$_j$)	2178
Crossflow Reynolds number (Re$_c$)	570000
Jet Reynolds number (Re$_j$)	14000

NUMERICAL METHODS

In this section, a brief overview on the numerical models employed in the present work is reported in order to study the two-phase flow under investigation.

In the E-E model derived from ELSA model, the two phase flow is analysed as a single phase flow composed of two species with highly variable density. Therefore, beyond the equation for the mixture momentum, the solver essentially consists of an equation for the liquid volume fraction (α_1) to predict the liquid evolution and of an equation for liquid/gas interface per unit of volume (Σ) to model the breakup process and to consider a polydisperse spray distribution. These two equations are reported below. It

is worth noting that locally the spray Sauter Mean Diameter (SMD) can be directly calculated from α_1 and Σ as $SMD = 6\,\alpha_1/\Sigma$.

$$\frac{\partial \alpha_1}{\partial t} + \frac{\partial U_i \alpha_1}{\partial x_i} = -\frac{\partial R_{\alpha_1,i}}{\partial x_i} = \frac{\partial}{\partial x_i}\left(\frac{\nu_t}{Sc_t}\frac{\partial \alpha_1}{\partial x_i}\right) \qquad (1)$$

$$\frac{\partial \Sigma}{\partial t} + \frac{\partial U_i \Sigma}{\partial x_i} = \frac{\partial}{\partial x_i}\left(\frac{\nu_t}{Sc_t}\frac{\partial \Sigma}{\partial x_i}\right) + S_\Sigma \qquad (2)$$

where U represents the mixture velocity, ν_t the turbulent viscosity (i.e. the subgrid contribution in LES context), Sc_t the turbulent Schmidt number and S_Σ is the source term for Σ equation that accounts for primary breakup phenomena. The reader interested in a detailed description of the mathematical derivation of Σ equation and in particular of S_Σ is addressed to references Vallet and Borghi [10] and Lebas et al. [11]. The most important modelling strategy behind ELSA, in addition to the equation for Σ, is the exploitation of a gradient closure for the turbulent liquid flux ($R_{\alpha_1,j}$) inside the liquid volume fraction equation (see Equation (1)). The same hypothesis is used also in Equation 2 for Σ. However, such closure can be theoretically applied only in absence of a mean slip velocity ($\overline{U}_{slip}$) between the two phases (Andreini et al. [8], Lebas et al. [11]). This is not generally true for aero-engine applications where the liquid is subjected to high shear stresses due to the gas phase and, mainly at idle operating conditions, this can lead to strong differences of phase velocities (Andreini et al. [8]).

In order to overcome such limitation, a QME solver has been developed from ELSA introducing the effects of the most important liquid/gas interactions. Indeed, an innovative second order closure for $R_{\alpha_1,i}$ is proposed starting from the consideration that two main contributions can be determined (see Andreini et al. [8] and references therein) for the turbulent liquid flux:

- U_{slg}, that is the average relative velocity between the particle and the surrounding flow in the vicinity of the interface, which is directly related to the drag force acting on the liquid. The transport of liquid associated to this velocity is denoted as Ψ_{slg}.

- V_{Dlg}, that is the drift velocity. It is the conditional average of the fluid turbulent velocity fluctuations with respect to the particle distribution. The transport of the liquid associated to this velocity is denoted Ψ_{Dlg}.

In QME framework the drift flux is modelled using a gradient closure, consistenly with single phase flow approaches (see Andreini et al. [8] and references therein)., whereas Ψ_{slg} is calculated through a dedicated transport eqution. For the sake of brevity, the mathematical modelling is not described in detail here. Yet, the reader interested in the derivation of the equation for Ψ_{slg} is addressed to
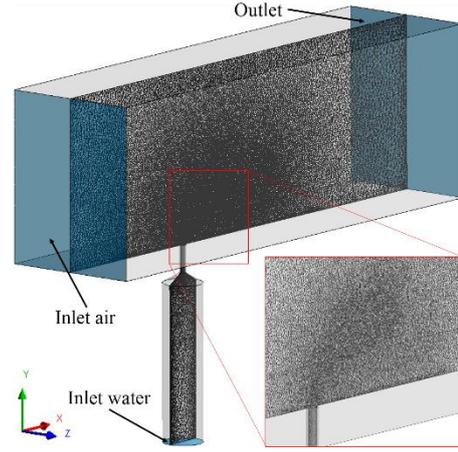

Figure 2: Sketch of the computational domain.

reference Andreini et al. [8], where the model is thoroughly presented.

Therefore, from a mathematical point of view, the QME becomes equivalent to a classical multiphase E-E solver, since the velocity of each phase can be directly deduced from the mixture velocity and the turbulent liquid flux. Nevertheless, it avoids the selection of which phase should be considered as discrete, allowing to model all ranges from a continuous phase to a dilute spray.

Furthermore, a Volume of Fluid phase-fraction approach (Rusche [12]) has been also considered in the present work in order to complete the comparison between the presented E-E models and an interface capturing method.

With regard to the turbulence modelling a LES spatial filter has been applied to the presented governing equations, where the sub-grid stress tensor has been modelled through a standard Smagorinsky closure.

NUMERICAL SETUP

Calculations here reported have been realized using OpenFOAM v. 3.0.1 considering, as already said, ELSA, QME and VoF approaches for liquid phase modelling. Simulations have been carried out on the computational domain reported in Figure 2. The domain dimensions, already used in Andreini et al. [8] are smaller than in the experiments. As shown in Herrmann et al. [13,14], where a Refined Level Set Grid (RLSG) method is used to track the liquid/gas interface for the same test case, this should not affect the obtained results. In order to correctly predict the jet behaviour and reproduce the effects of the *vena contracta*, the liquid pipe is included inside the computations.

A sensitivity analysis was carried out to define the most appropriate mesh sizing. Two different grids were generated with ANSYS ICEM-CFD and consist of tetrahedrons with a layer of 5 prisms close to the wall. The mesh sizing (in the mixing region) of the two grids are different, as highlighted in Table 2.

Table 2: Details of the computational grids.

Mesh	Hole region [mm]	Mixing sizing [mm]	Elements
M1	0.15	0.30	2.84e6
M2	0.15	0.15	9.50e6

Mass flow rates are imposed at the inlets of both air and water following data reported in Table 1, whereas a static pressure is prescribed at the outlet. All the walls are treated as smooth, non-slip and adiabatic, whereas the upper and the lateral surfaces are considered slip walls as done also in (Herrmann et al. [14]).

The time step (dτ) used for the simulations has been chosen in order to ensure a control of the Courant number inside the computational domain. Therefore, calculations were performed with 1e-7 s for the coarser mesh while dτ has been reduced to 8e-8 s for M2. However, in simulations employing the QME approach, because of the high coupling between the equations for liquid volume fraction, turbulent liquid flux and liquid/gas interface density, the time step for the coarser mesh has been slightly reduced to 8e-8 s to avoid numerical instabilities.

Given that the hereby studied geometry is 0.65m long and that the average speed between liquid and gas is 50 m/s, a flow-through time of 0.0013 s crossing time can be calculated. Hence, after an initialisation period of 2 flow-through times required to flush out the initial conditions and to allow the underlying flow field to develop, the statistics were collected over 4.0 flow-through times.

All the solvers employed follow a classical segregated method called PIMPLE, which is based on a PISO loop within a SIMPLE loop to solve the pressure-velocity coupling. Thanks to the small time step employed, 3 internal corrector steps have been used in the present computations in order to achieve the coupling between continuity and momentum and 3 external loops. Moreover, both convective and diffusive fluxes have been discretized following second order schemes whereas a second order implicit Euler scheme has been employed for time advancement.

RESULTS AND DISCUSSION

ELSA approach

The ELSA model was firstly used to determine the most appropriate mesh sizing for the following simulations, where different formulations for the two-phase modelling were tested. The instantaneous velocity fields obtained with the two different grids are reported in Figure 3.

As expected, the spatial discretization seems beneficial in reducing the scale of the resolved turbulent vortices in the mixing region. However, the structure of the jet immediately downstream of the hole appears rather uninfluenced, at least from a qualitative point of view.

In order to obtain a quantitative validation, the results were evaluated in terms of time-averaged jet penetration which, according to Brown and McDonell [9], was evaluated as the trajectory of the outer side of the jet and plotted as a function of direction x (distance from the centre of the hole in the downstream direction). In the numerical
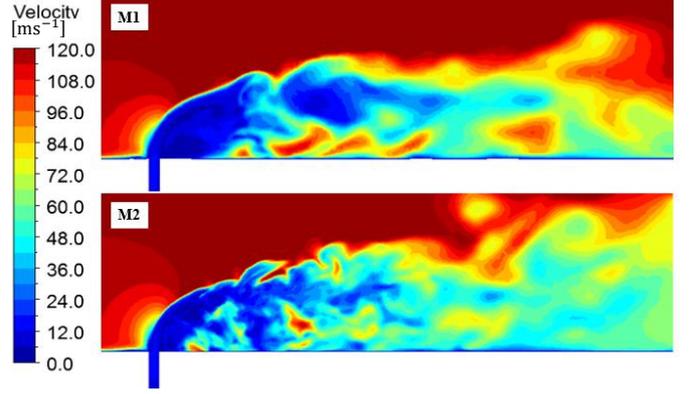

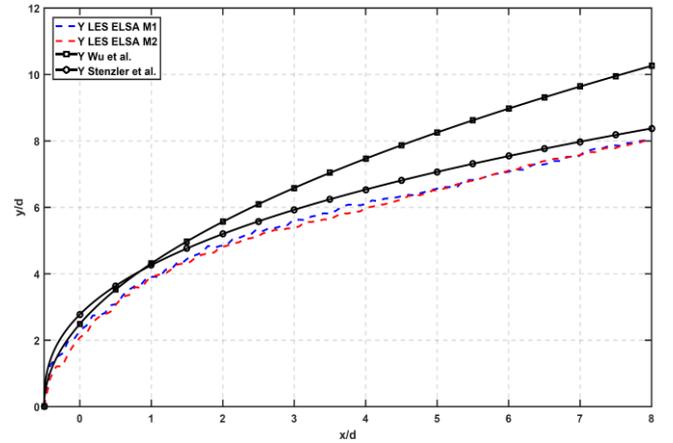**Figure 3: Instantaneous velocity field.**

Figure 4: Mean jet penetration between different grids M1 and M2.

simulations, the position of the upper edge was calculated accordingly to a previous work on the same test case where such aspect is discussed in detail (Andreini et al. [8]). The outer jet trajectories obtained with the two grids are plotted in Figure 4, where results are compared against two correlations published in literature by Wu et al. [15] and Stenzler et al. [16], shown respectively in equations 3 and 4.

$$\frac{y}{d} = 1.37 \left(q \frac{x}{d} \right)^{0.5} \qquad (3)$$

$$\frac{y}{d} = 2.63 q^{0.442} \left(\frac{x}{d} \right)^{0.39} We_c^{-0.088} \left(\frac{\mu_l}{\mu_{H_2O}} \right)^{-0.027} \qquad (4)$$

where d represents the jet diameter while μ_l and μ_{H_2O} are respectively the viscosity of the analysed liquid and a reference value for water.

From this comparison it is possible to draw some interesting considerations: it appears that the resulting penetration is insensitive to the increasing mesh refinement, at least in time-averaged terms. In the light of these results, only the coarse mesh (M1) will be shown hereafter, since the slight difference in jet penetration does not justify the significant increase in computational cost ascribed to the

combination of greater number of elements and smaller time step required.

In addition, it is also worth pointing out the slight underestimation of results obtained with the ELSA approach compared to the correlation by Stenzler et al. [16], which, according to Brown and McDonell [9] provided the best fitting with the experimental data.

To better appreciate the capability of CFD to reproduce the jet behaviour, the simulations were post-processed to allow a comparison against the experimental acquisitions obtained through high speed shadowgraphy. However, due to the strong presence of light scattering, reproducing the actual physical process involved in the image acquisition is not straightforward. To model the shadowgraphy technique, the turbidimetry theory is used to quantify the loss of light intensity (I) due to the scattering effect ascribed to suspended particles. Hence, considering the spray as locally monodisperse and applying the Beer-Lambert law, it is possible to express the variation of I along a given path of length L (the lateral direction y in this particular case) as the line integral of the product between the particle volume concentration (N_d), the squared Sauter Mean Diameter and an extinction coefficient (Q_{ext}), which in the present study has been evaluated equal to 2 (see Xiao-Shu et al. [17] and Ren et al. [18] for further details). It is possible to prove that such expression can be reformulated as a function of the liquid/gas interface density Σ, as highlighted in Equation 5.

It is worth underlining that the present approach is based on spray characteristics and therefore can be considered valid only when the spray is diluted (i.e. not for a coherent liquid jet). Therefore, the dense spray region in the present work has been identified considering values of liquid volume fraction higher than 10% (i.e. where a dilute assumption is no more verified) and assigning a constant value to the integral kernel.

$$\left(\frac{I}{I_0}\right) = \exp\left(-\int_0^L Q_{ext} N_d \frac{\pi D_{32}^2}{4} dl\right) = \exp\left(-\int_0^L \frac{\Sigma}{2} dl\right) \quad (5)$$

The application of this procedure allows to obtain the liquid distribution depicted in Figure 5 for mesh M1. The liquid column, which can be clearly identified in the near injector region, due to instabilities generated by the interactions with the gas phase, tends to be firstly atomized in bigger liquid structures until a broad range of drop sizes (i.e. Σ) is generated. In the experimental window shown in blue on the top part of Figure 5, a comparison with the experimental picture is reported (for the sake of clarity, the result of the ELSA simulation has been coloured in red). This representation reveals again that the penetration is not properly predicted mainly after x/d > 1.0 and this is probably due to the hypothesis of zero slip velocity between phases. Indeed, once the liquid rupture begins, generated droplets and liquid structures, due to their high inertia, tend to follow different trajectories before relaxing to the dynamics of the carrier phase. This fact leads locally to important differences between liquid and gas velocity.
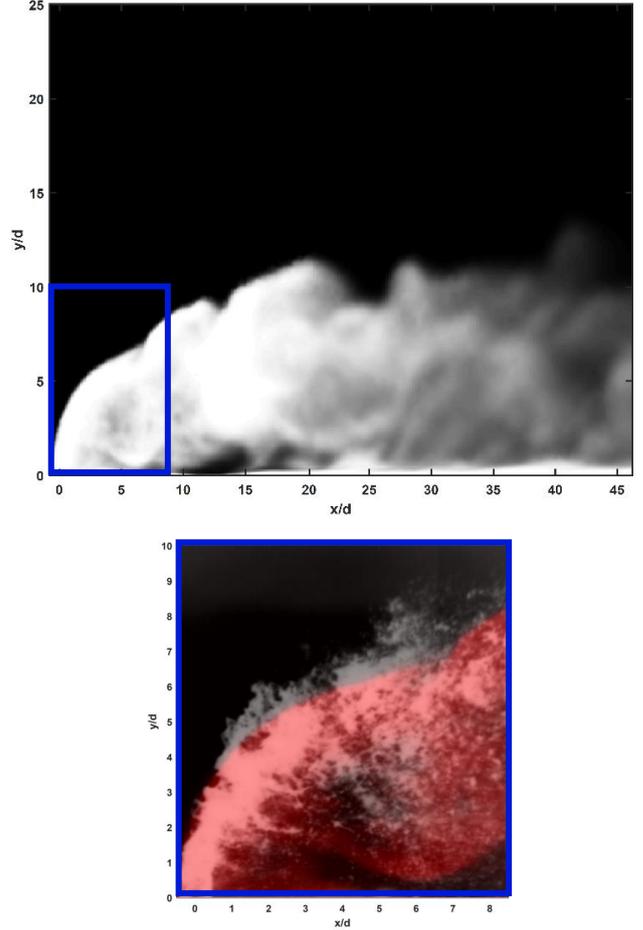

Figure 5: Liquid distribution obtained from ELSA calculations compared with experiments

Furthermore, the simulation is not correctly catching the liquid wrinkling due to the gas phase interactions. However, this is consistent with the ELSA approach that is not an interface-capturing method. Moreover, in the present work, any modelling effort has been prompted to describe the liquid-gas surface at subgrid level. Adaptive mesh refinement (Fuster et al. [19]), subgrid level set method (Herrmann et al. [14]) or subgrid models (Chesnel et al. [20]) should be used to this end, but they still represent an open issue and their investigation goes beyond the goal of the present study. Further developments are required on this aspect.

However, a further confirmation of the reliability of the LES-ELSA approach can be obtained evaluating the breakup location of the liquid column. To this end, Figure 6 reports the instantaneous evolution of Σ zoomed in the near injector region. It is worth pointing out that a production of Σ, which is related to the generation of some instabilities on the liquid column surface due to the interactions with the gas crossflow, is determined on the top and bottom side of the water jet. Clearly, such production is much higher on the top jet surface since the gas phase has a stronger impact on the liquid evolution. Going downstream, the point where these two sides of Σ connect together has been defined in the present work as the location of the liquid column breakup.
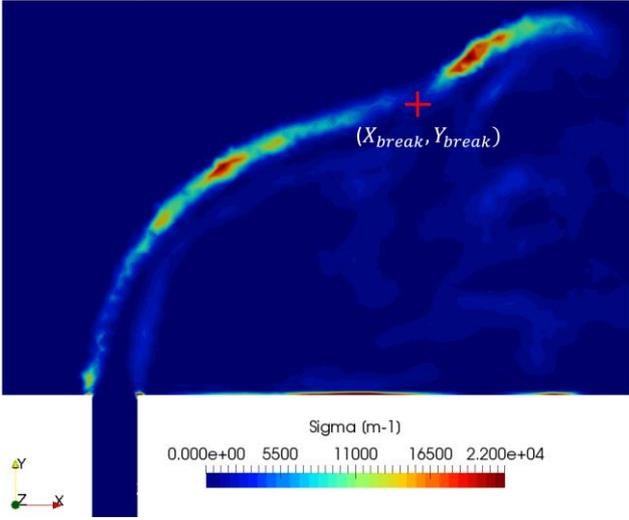
5

Figure 6: Distribution of the liquid/gas interface (Σ) obtained from ELSA computations.

Figure 7: Mean jet penetration obtained with several modelling strategies for liquid phase modelling.

It should be pointed out that, immediately after such point, a strong production of Σ is predicted and such thing is related to the generation of some detached liquid structures. The location of the liquid column breakup has been compared with the following experimental correlation proposed by Wang et al. [21], where the breakup dynamics of a plain liquid jet in air crossflow is studied.

$$\frac{X_{breakup}}{d} = 6.9 \qquad (6)$$

$$\frac{Y_{breakup}}{d} = 2.5q^{0.53} \qquad (7)$$

The correlation, valid for a wide range of operating conditions and momentum flux ratios, gives the position of the column disintegration point as a function of the momentum flux ratio and of the jet diameter. It is possible to notice that ELSA is physically reproducing the breakup length.

VoF and QME approaches

Once evaluated and described in detail the main characteristics of ELSA approach, the attention was diverted to the other modelling strategies. As already stated, the objective of this benchmark is the assessment of the potential advantages of the proposed QME formulation over the ELSA model, using VoF as reference solution.

Firstly, the resulting mean jet trajectory is plotted in Figure 7, where it is possible to appreciate the good agreement shown by VoF in reproducing the correlation by Stenzler et al. [16]. The enhancements with respect to ELSA can be determined immediately after x/d>0, where the exploitation of an interface capturing method leads to a physical prediction of the jet penetration. Even more important, it is evident how the introduction of a more reliable description of the slip velocity (i.e. QME plot results) between the two phases allows to increase the jet
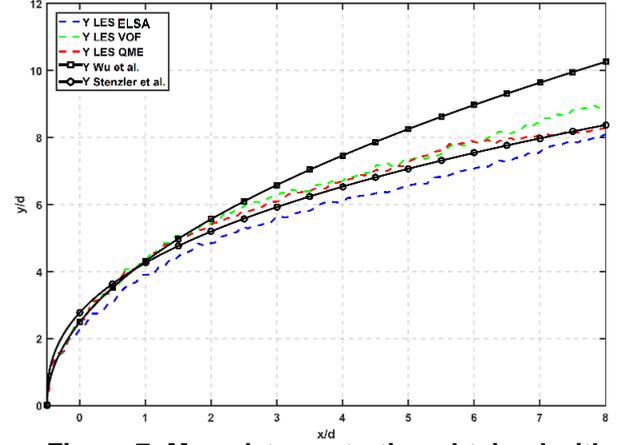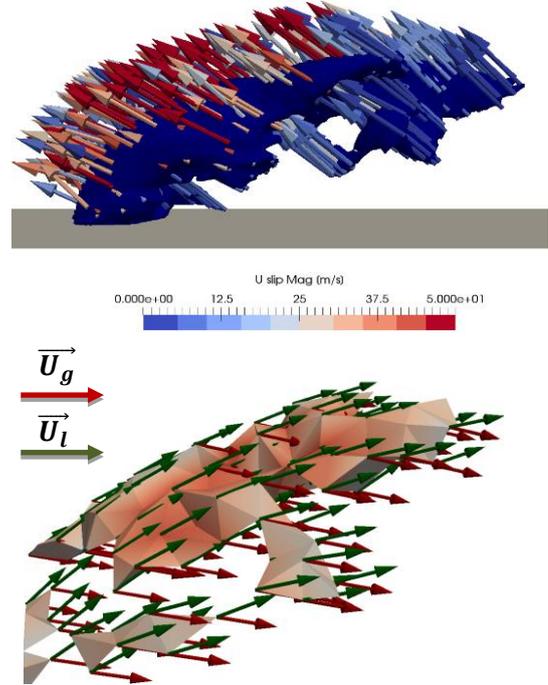

Figure 8: Slip velocity effect on liquid distribution (top) and vectorial comparison between liquid and gas velocity (bottom).

penetration coherently with VoF.

Indeed, in the top part of Figure 8, the iso-surface of 5% of liquid volume fraction superimposed on the slip velocity field shows that the difference of velocity between phases tends to lift up the jet and such effect is mainly generated in the region where the two jets collide due the inertia of the liquid phase. The instantaneous velocity vector representation of the liquid and gas velocities on the isosurface corresponding to the maximum value of slip velocity (i.e. in the region where the two jets collide), reported on the bottom of the same figure, proves that such $\vec{U}_{slip}$ cannot be neglected since it is evident that liquid and gas continue to follow different trajectories while interacting with each other.. Then, moving downstream, the slip

velocity is gradually reduced by the drag contribution until it becomes zero based on the local distribution of the SMD and relaxation times.

Considering the comparison with experiments with the same procedure shown in Figure 5, it is possible to appreciate an improvement in the prediction of the liquid distribution with respect to ELSA (see Figure 9).

Obviously, the proposed post processing tool is directly relevant only for QME, for which the information about the liquid/gas interface density is available. Whereas for VoF, an iso-surface of 5% of liquid volume fraction has been chosen for a qualitative comparison.
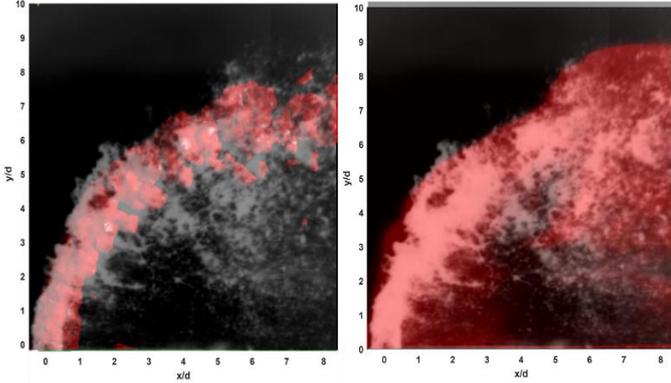

Figure 9: Liquid distribution obtained from VOF (left) and QME (right) calculations compared with experiments.

It is clear that, using an interface-capturing method, the penetration and the jet behaviour immediately after the jet entrance seem physically predicted. Yet, due to a computational domain not refined enough to correctly reconstruct the interface (especially when breakup phenomena appear), the subsequent column breakup is roughly represented and the liquid volume fraction field undergoes an excessive numerical diffusion. Therefore, in VoF framework the best prediction with respect to ELSA is due to a non-realistic representation of the atomisation process because all the scales of the interface are not well resolved. To overcome this problem, a highly refined mesh would be required, as shown for instance in Herrmann et al. [13,14], but this is outside the scope of the present work.

Instead, the QME approach can be seen as a good compromise between computational cost and simulation accuracy, since a prediction of penetration and a global jet behaviour in the near injection region consistent with a VoF method has been obtained, but with the further opportunity of evaluating the subsequent jet breakup with a reduced computational cost.

In addition to the mean penetration, the jet oscillation has been analysed using the experimental acquisition shown in Figure 1 as reference. Considering that no details were provided in Brown and McDonell [9] regarding the measurement of the standard deviation of the penetration, in the present work the root mean square of the liquid volume fraction field has been chosen to identify the jet unsteadiness.
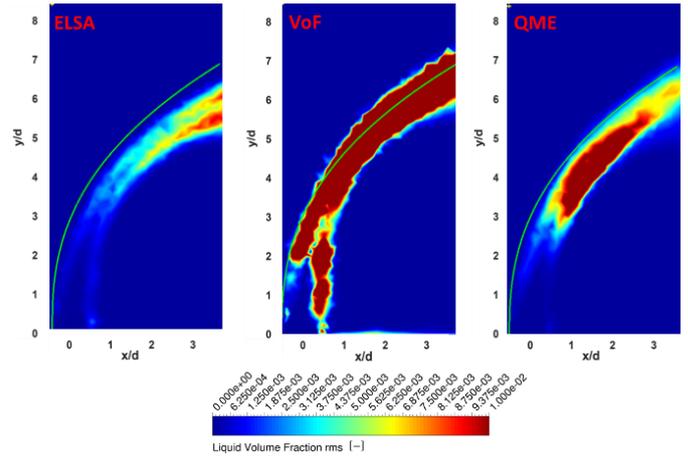

Figure 10: Standard deviation of liquid volume fraction obtained with ELSA, VoF and QME approaches.

In Figure 10 such quantity is shown for each employed E-E method and compared with the experimental correlation (i.e. the green curve) for mean penetration reported in Equation 4.

Consistently with the experimental behaviour, VoF, which exploits an interface-capturing method seems to oscillate around the experimental penetration whereas ELSA predicts a liquid volume fraction fluctuation on a lower position (i.e. coherently with Figure 7). Indeed, considering VoF as the reference solution, in ELSA the higher numerical diffusion together with the exploitation of a first order closure for turbulent liquid flux leads to a non-physical representation of liquid-gas interactions and to a strong underestimation in the liquid volume fraction fluctuations.

QME, including the contribution of slip velocity inside the liquid volume fraction equation, leads to modify the jet behaviour and therefore also the resulting standard deviation. The resolution of the turbulent liquid flux contribution reduces the liquid diffusion and leads to appreciate higher rms values immediately after jet exit. The results are more consistent with VoF even if QME does not still oscillate exactly around the experimental penetration. This can be justified by fact that the proposed approach involves the introduction of only the effects of a mean slip velocity between phases inside the liquid volume fraction equation. But, the impact of the drift flux is still calculated through a gradient closure as explained in the section dedicated to numerical modelling. This modelling strategy is probably determining a too high numerical diffusion, that is lowering the α_1 fluctuations with respect to the interface capturing method.

CONCLUSIONS

The present study has been carried out with the main aim of evaluating the performances of QME approach in LES framework on a jet in crossflow test case with a direct comparison against other available E-E approaches and experimental data. The proposed approach is an improvement of the Eulerian-Eulerian model derived from

ELSA and it exploits a second order closure for turbulent liquid flux to account for the slip velocity between liquid and gas. This method fills the gap between mixture E-E models and classical two-phase approaches with the important possibility of addressing both dense and dispersed flow regions.

Firstly, LES results obtained with ELSA have been considered to compare jet mean penetration against experimental data. Then, an advanced post processing analysis, based on turbidimetry theory, has been proposed to obtain a 2D image consistent with experimental visualization. Even if ELSA seems able to physically reconstruct the global jet behaviour in terms of breakup length, the jet penetration is not properly predicted and this is probably due to the hypothesis of zero slip velocity between phases used in the liquid volume fraction equation. To overcome such inconveniences, QME performances are presented in the second part of the paper and compared with an interface capturing approach. It has been shown that such proposed second order E-E model allows to better appreciate liquid distribution both in terms of mean penetration and jet oscillation. However, even if QME and VoF lead to similar results in the near injector region, the mesh resolution used in VoF is not fine enough to properly appreciate the subsequent jet breakup and would require a mesh refinement to reduce the numerical diffusion in the downstream region as well as to determine the main characteristics of the generated spray. Instead, QME, exploiting the equation of Σ, is able to account also for unresolved liquid structures, leading to a robust and reliable solver on an industrial perspective capable of including the slip velocity between phases. However, the chosen test case is lacking in terms of spray measurements and therefore the present work can be considered just as a preliminary validation of the proposed approach. Further developments are expected on additional and more detailed experimental rigs. In this context, the exploitation of a coupled strategy VoF-QME, able both to solve the interface evolution and to reconstruct the subsequent spray generation, is also expected.

NOMENCLATURE

d	Jet diameter	[m]
I	Light intensity	[lm]
q	Momentum flux ratio	[-]
N	Volume concentration	[-]
Q_{ext}	Coefficient of extinction	[-]
Re	Reynolds number	[-]
R_{α_1}	Turbulent liquid flux	[ms^{-1}]
SMD	Sauter Mean Diameter	[m]
t	Time	[s]
x	Crossflow direction	[m]
y	Jet inflow direction	[m]
z	Lateral direction	[m]
U	Velocity	[ms^{-1}]
We	Weber number	[-]

Greeks

α_1	Liquid volume fraction	[-]
Σ	Liquid-gas interface density	[m^{-1}]
μ	Dynamic viscosity	[Pa/s]
σ	Surface tension	[Nm^{-1}]

Subscripts

c	Crossflow
d	Droplet
g	Gas
H_2O	Water reference value
j	Jet
l	Liquid

Acronyms

CFD	Computational Fluid Dynamics
CAEP	Committee on Aviation Environmental Protection
DQMOM	Direct Quadrature Method of Moments
ELSA	Eulerian-Lagrangian Spray Atomization
LES	Large Eddy Simulation
QME	Quasi Multiphase Eulerian
QMOM	Quadrature Method of Moments
RANS	Reynolds-Averaged Navier-Stokes
rms	Root Mean Square
VoF	Volume of Fluid

REFERENCES

[1] ICAO, 2010, "Enviromental report, aviation and climate change."

[2] Williams, FA, "Spray Combustion and Atomization", Phys. Fluids 1958-1988, 1(6), 1958, pp. 541–545.

[3] Laurent, F, and Massot, M, "Multi-fluid modelling of laminar polydisperse spray flames: origin, assumptions and comparison of sectional and sampling methods", Combust. Theory Model., 5(4), 2001, pp. 537–572.

[4] Marchisio, D L, Pikturna, JT, Fox, RO, Vigil, RD, and Barresi, AA, "Quadrature method of moments for population-balance equations", AIChE J., 49(5), 2003, pp. 1266–1276.

[5] Fox, RO, Laurent, F, and Massot, M, "Numerical simulation of spray coalescence in an Eulerian framework: Direct quadrature method of moments and multi-fluid method", J. Comput. Phys., 227(6), 2008, pp. 3058–3088.

[6] Massot, M, "Eulerian Multi-Fluid Models for Polydisperse Evaporating Sprays", Multiphase Reacting Flows: Modelling and Simulation, D.L. Marchisio, and R.O. Fox, eds., Springer Vienna, 2007, pp. 79–123.

[7] Vié, A, Jay, S, Cuenot, B, and Massot, M, "Accounting for Polydispersion in the Eulerian Large Eddy

Simulation of the Two-Phase Flow in an Aeronautical-type Burner", Flow Turbul. Combust., 90(3), 2013, pp. 545–581.

[8]   Andreini, A, Bianchini, C, Puggelli, S, and Demoulin, FX, "Development of a turbulent liquid flux model for Eulerian–Eulerian multiphase flow simulations", Int. J. Multiph. Flow, 81, 2016, pp. 88–103.

[9]   Brown, CT, and McDonell, VG, "Near Field Behavior of a Liquid Jet in a Crossflow", ILASS Americas 19th Annual Conference on Liquid Atomization and Spray Systems, Toronto, Canada, 2006.

[10]   Vallet, A, and Borghi, R, "Modélisation eulerienne de l'atomisation d'un jet liquide", Comptes Rendus Académie Sci. - Ser. IIB - Mech.-Phys.-Astron., 327(10), 1999, pp. 1015–1020.

[11]   Lebas, R, Menard, T, Beau, PA, Berlemont, A, and Demoulin, FX, "Numerical simulation of primary break-up and atomization: DNS and modelling study", Int. J. Multiph. Flow, 35(3), 2009, pp. 247–260.

[12]   Rusche, H, "Computational Fluid Dynamics of Dispersed Two-Phase Flows at High Phase Fractions", PhD thesis, Imperial College, 2002.

[13]   Herrmann, M, "Detailed Numerical Simulations of the Primary Atomization of a Turbulent Liquid Jet in Crossflow", J. Eng. Gas Turbines Power, 132(6), 2010.

[14]   Herrmann, M, Arienti, M, and Soteriou, M, "The Impact of Density Ratio on the Liquid Core Dynamics of a Turbulent Liquid Jet Injected Into a Crossflow", J. Eng. Gas Turbines Power, 133(6), 2011.

[15]   Wu, PK, Kirkendall, KA, Fuller, RP, and Nejad, AS, "Breakup Processes of Liquid Jets in Subsonic Crossflows", J. Propuls. Power, 13(1), 1997, pp. 64–73.

[16]   Stenzler, JN, Lee, JG, Santavicca, DA, and Lee, W, "Penetration of Liquid Jets in a Cross-flow", At. Sprays, 16(8), 2006.

[17]   Xiao-Shu, C, Nai-Ning, W, Jing-Ming, W, and Gang, Z, "Experimental investigation of the light extinction method for measuring aerosol size distributions", J. Aerosol Sci., 23(7), 1992, pp. 749–757.

[18] Ren, KF, Xu, F, Dorey, JM and Cai, X, "Development of a precise and in situ turbidity measurement system", Proc. AIP: Multiphase flow: the ultimate measurement challenge, ed. X. S. Cai, Y. X. Wu, Z. Y. Huang, S. M. Wang and M. Wang, 2007, vol. 1: 490-495.

[19]   Fuster, D, Bagué, A, Boeck, T, Le Moyne, L, Leboissetier, A, Popinet, S, Ray, P, Scardovelli, R, and Zaleski, S, "Simulation of primary atomization with an octree adaptive mesh refinement and VOF method", Int. J. Multiph. Flow, 35(6), 2009, pp. 550–565.

[20]   Chesnel, J, Reveillon, J, Menard, T, and Demoulin, FX, "Large Eddy Simulation of Liquid Jet Atomization", At. Sprays, 21(9), 2011.

[21]   Wang, Q, Mondragon, U M, Brown, C T, and McDonell, V G, "Characterization of trajectory, break point, and break point dynamics of a plain liquid jet in a crossflow", At. Sprays, 21(3), 2011.